iScience

CellPress
OPEN ACCESS

Article

Differential response of C9orf72 transcripts following neuronal depolarization

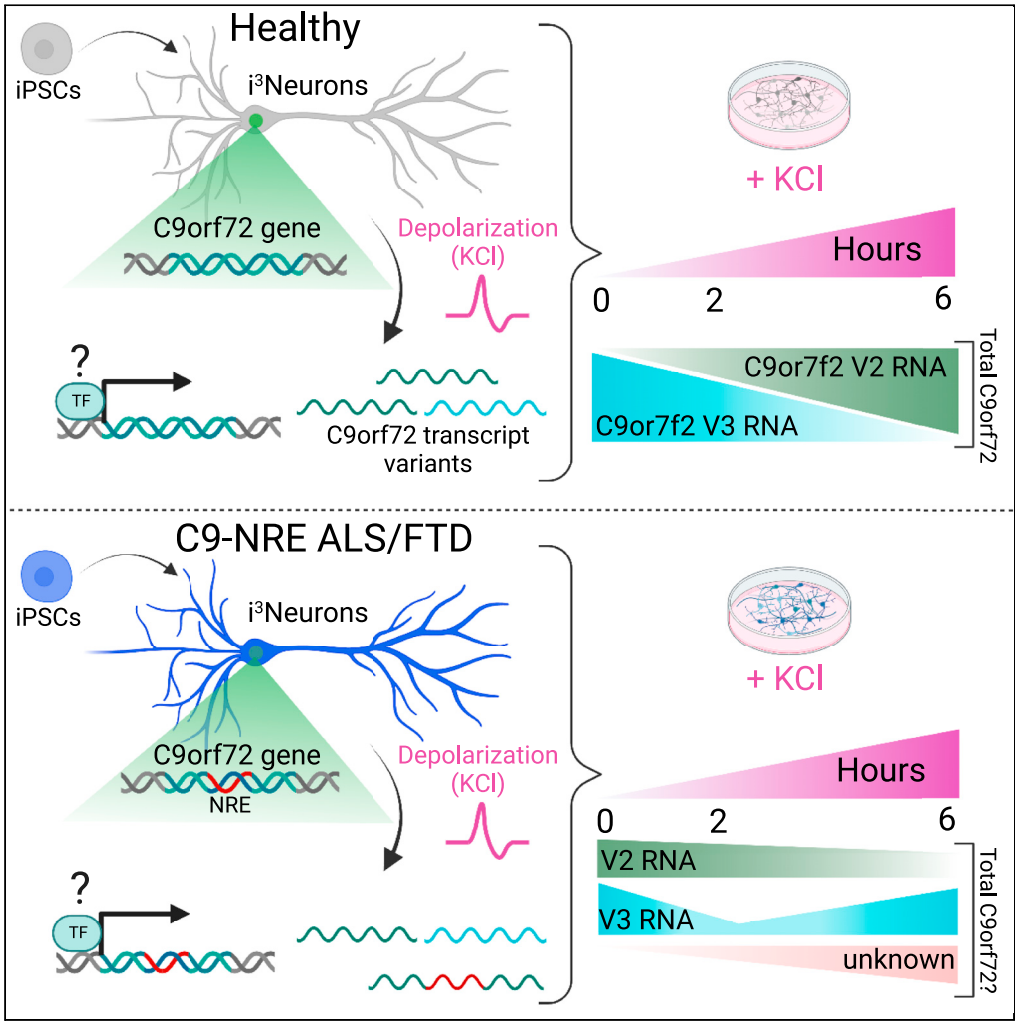

Layla T. Ghaffari, Davide Trotti, Aaron R. Haeusler

aaron.haeusler@jefferson.edu

Highlights

Neuronal depolarization regulates C9orf72 levels

Prolonged membrane depolarization downregulates C9orf72 V3

C9-NRE carriers do not show the same response to depolarization

Ghaffari et al., iScience 26, 106959
June 16, 2023
https://doi.org/10.1016/j.isci.2023.106959

iScience

CellPress
OPEN ACCESS

Article

Differential response of C9orf72 transcripts following neuronal depolarization

Layla T. Ghaffari,[1] Davide Trotti,[1] and Aaron R. Haeusler[1,2,*]

SUMMARY

The $(G_4C_2)_n$ nucleotide repeat expansion (NRE) mutation in C9orf72 is the most common genetic cause of ALS and FTD. The biological functions of C9orf72 are becoming understood, but it is unclear if this gene is regulated in a neural-specific manner. Neuronal activity is a crucial modifier of biological processes in health and neurodegenerative disease contexts. Here, we show that prolonged membrane depolarization in healthy human iPSC-cortical neurons leads to a significant downregulation of a transcript variant 3 (V3) of C9orf72, with a concomitant increase in variant 2 (V2), which leads to total C9orf72 RNA transcript levels remaining unchanged. However, the same response is not observed in cortical neurons derived from patients with the C9-NRE mutation. These findings reveal the impact of depolarization on C9orf72 transcripts, and how this response diverges in C9-NRE-carriers, which may have important implications in the underlying unique clinical associations of C9-NRE transcripts and disease pathogenesis.

INTRODUCTION

The nucleotide repeat expansion (NRE), $(G_4C_2)_n$, which is located in a classically non-coding region of the C9orf72 (C9) gene, is the most common genetic cause of two progressive neurodegenerative diseases, amyotrophic lateral sclerosis (ALS) and frontotemporal dementia (FTD).[1,2] This disease-causative mutation in C9 is associated with three non-mutually exclusive pathogenic mechanisms: (1) The NRE is transcribed into repeat-containing RNA in sense and anti-sense directions, which can sequester RNA-binding proteins that are critical for cellular homeostasis,[3–7] (2) the repeat-containing RNA is aberrantly translated via a mechanism called repeat-associated non-AUG (RAN) translation, leading to the production of dipeptide repeat proteins (DPRs) that can be neurotoxic,[8–10] (3) the presence of the NRE in C9orf72 leads to a reduction of transcript levels and thus can then lead to a loss of C9orf72 protein levels and haploinsufficiency.[2,4,11] Although the direct contribution of C9orf72 loss-of-function to neurodegeneration is unclear, global ablation of C9orf72 in mice leads to inflammatory states in the periphery and CNS,[12–14] the C9orf72 protein has been shown to be involved in several cellular processes that are essential to neuronal survival and function. For example, C9orf72 is localized to lysosomes[15]; is found at synapses[16–18]; interacts with synaptic proteins and regulates excitatory synapse number[19]; acts as a guanine nucleotide exchange factor[20]; and is involved in intracellular membrane trafficking.[21] Furthermore, there is increasing evidence that the C9orf72 gene plays a role in maintaining synaptic homeostasis.[19,22] Although some efforts have advanced our understanding of the regulation of the C9orf72 gene locus in a healthy context,[23] there are still fundamental unanswered questions regarding the regulation of the C9orf72 gene expression in neurons and the role this may play in neurodegenerative disease.

Many biological processes are modified in response to changes in neuronal activity in the context of both health and disease settings.[24–27] Processes such as transcription,[24,25,28] chromatin accessibility,[29] methylation,[30,31] receptor trafficking,[32] and survival[33] are influenced by levels and patterns of neuronal firing. Abnormal neuronal activity is linked to many neurological diseases,[26,34] including ALS. Cortical hyperexcitability is a commonly conserved feature of many subtypes of ALS, independent of disease etiology, and is often observed early in disease progression before degeneration of the corticospinal tract and involvement of motor neurons.[35–40] A possible relationship between neuronal activity and the pathomechanisms associated with the NRE is becoming clearer. It has been shown that increased excitatory neuronal activity via Channelrhodopsin-2 or excess glutamate increases levels of dipeptide repeat proteins (DPRs) in primary rat

[1]Jefferson Weinberg ALS Center, Vickie and Jack Farber Institute for Neuroscience, Department of Neuroscience, Thomas Jefferson University, Philadelphia, PA 19107, USA

[2]Lead contact

*Correspondence: aaron.haeusler@jefferson.edu

https://doi.org/10.1016/j.isci.2023.106959

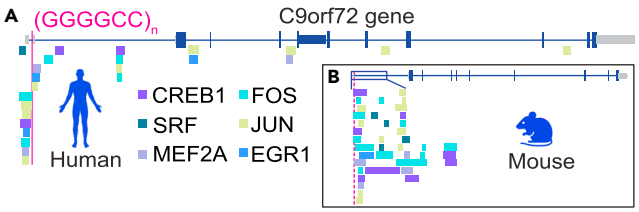

Figure 1. Activity-dependent transcription factors are enriched near the promoter region of the C9orf72 gene locus in humans and rodents

(A) Visualization of peaks from ChIP-seq data from the ENCODE project on the UCSC Genome Browser, which was filtered for known activity-dependent transcription factor peaks on the human C9orf72 gene. The red line denotes the location of the NRE gene mutation found in ALS/FTD patients.

(B) Visualization of peaks of activity-dependent transcription factors from ChIP-seq data from ReMap on the UCSC Genome Browser in the mouse C9orf72 homolog (3110043O21 Rik). The red dotted line denotes the repeat-like region in the mouse homolog.

cortical neurons and C9-ALS/FTD patient-derived human induced pluripotent stem cells (hiPSC) differentiated into motor neurons.[41,42] Understanding the relationship between neuronal activity and the C9orf72 gene locus in healthy and disease contexts will be important to further elucidate the dynamics between loss and/or gain of function disease mechanisms associated with the C9-NRE mutation.

Here, we dissect the relationship between neuronal depolarization and the expression of C9orf72 transcripts. We used rodent cortical neurons and human induced pluripotent stem cells (hiPSCs) differentiated into glutamatergic cortical-like neurons (i^3Neurons[43,44]). Neuronal depolarization via potassium chloride (KCl) bath, which uniformly, synchronously, and sustainably increases levels of intracellular calcium, reduces C9orf72 RNA in rat cortical neurons, despite the promoter being enriched for known activity-dependent transcription factors. In i^3Neurons from healthy individuals, neuronal depolarization leads to a significant decrease in the C9orf72 transcript variant 3 (V3), in which the repeat region is located in the intronic region. Furthermore, to determine if these observations regarding C9orf72 levels following neuronal depolarization hold true in a disease context, we utilized C9-ALS/FTD patient-derived i^3Neurons (hereby called C9-NRE). Of interest, the same level of transcriptional downregulation of V3 in response to neuronal depolarization is not observed in C9-NRE i^3Neurons. These findings provide insight into the physiological expression of the C9orf72 transcripts under conditions of neuronal depolarization and how this regulation may be divergent in patients carrying the C9orf72 NRE mutation, which may have implications for disease pathogenesis.

RESULTS

The C9orf72 promoter is enriched with activity-dependent transcription factors in human and rodents

To determine if the C9orf72 gene is a candidate for neuronal activity-dependent transcriptional regulation, we first sought to determine if known activity-dependent transcription factors occupy the promoter region. To accomplish this, we examined publicly available chromatin immunoprecipitation (ChIP)-sequencing datasets from the Encyclopedia of DNA Elements (ENCODE)[45,46] and ReMap2022[47] on the UCSC Genome browser. Leveraging these datasets, we identified that both the human C9orf72 gene (Figure 1A) and the mouse C9orf72 gene homolog, 3110043O21Rik, (Figure 1B), are enriched for canonical activity-dependent transcription factors (TFs) near the annotated promoter regions for these genes in somatic and neural cells (original UCSC Genome Browser screenshot shown in Figure S1). These activity-dependent TFs play a role in the well-established biphasic temporal transcriptional response to neuronal activity. The first program of activity-dependent transcription, described here as the early wave, is the initial rapid response to neuronal stimulation that induces immediate-early genes (IEGs). Many IEGs are TFs that regulate the secondary program of activity-dependent transcription, described here as the late wave, which induces late response genes (LRGs). Specifically, CREB1, SRF, and MEF2A are upstream regulators of the first program of activity-dependent transcription, inducing the IEGs EGR1, FOS, and JUN (the latter two form the AP-1 complex), and are regulators of the secondary program (Figure 2B). The enrichment of these activity-dependent transcription factors indicates that the C9orf72 gene locus could potentially be responsive to changes on neuronal depolarization.

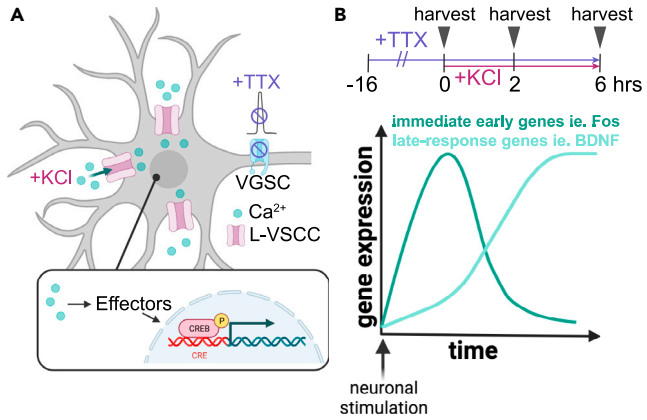

Figure 2. Schematic of experimental paradigms used in this study

(A) Neurons are silenced with 1 μM tetrodotoxin (TTX), which antagonizes voltage-gated sodium channels (VGSC) to quiet endogenous synaptic activity. Neurons are then depolarized with elevated levels of extracellular potassium chloride (KCl, 55 mM), which allows Ca^{2+} influx through L-type voltage-sensitive Ca^{2+} channels (L-VSCC). The Ca^{2+} influx acts on effector proteins that activate activity-dependent transcription factors such as CREB1, shown in the phosphorylated (active) form, which subsequently acts on target DNA.

(B) Neurons are silenced with TTX overnight (16 h) before KCl-induced depolarization. Timeline of TTX addition following KCl depolarization. Neurons are harvested at 0-, 2-, or 6-h post depolarization in line with the two waves of activity-dependent gene expression.

C9orf72 transcripts are reduced following K^+-induced neuronal depolarization in rat cortical neurons

To examine the impact neuronal depolarization has on the levels of C9orf72, we employed a widely used experimental paradigm to activate this pathway in rat primary cortical neurons.[25,48,49] In this paradigm, endogenous neuronal activity is silenced using 1 μM tetrodotoxin (TTX), which binds to and blocks voltage-gated sodium channels involved in action potential generation, and then subsequent membrane depolarization is driven by elevated levels of extracellular potassium chloride (55 mM, KCl) (Figure 2A). Silencing endogenous neuronal activity before depolarization ensures that neurons *in vitro* are simultaneously depolarized and the activity-dependent transcriptomic pathways are not being induced before stimulation. Although not a model of hyperactivity, this method ensures a high signal-to-noise ratio for the evoked activity-dependent molecular cascades following stimulation and yields high experimental control. This methodology to explore the causal relationship between neuronal depolarization and transcription has been extensively established and reviewed.[24,25,48] Briefly, membrane depolarization by KCl increases and sustains levels of intracellular calcium (Ca^{2+}), primarily through L-type voltage-sensitive Ca^{2+} channels (L-VSCC), which activates effectors such as Ca^{2+}/calmodulin-dependent protein kinase (CaMK),[50] mitogen-activated protein kinase (MAPK),[51] and calcineurin,[52,53] among others,[48] which then activate TFs, such as CREB, through phosphorylation, depicted in Figure 2A. Because the promoter of C9orf72 is occupied by TFs responsible for both early and late waves of activity-dependent transcription, we reasoned that C9orf72 could be an activity-dependent gene in either wave of the transcriptional response (Figure 2B). Therefore, we examined transcriptional responses to this experimental paradigm at time points consistent with the early and late waves of activity-dependent transcription; 2 h and 6 h, respectively (Figure 2B). Rat cortical neurons were used during synaptic and morphological maturity, day *in vitro* 21 (data not shown). We used the Ca^{2+} indicator Fluo-4 a.m. to measure the responses of rat primary cortical neurons exposed to this experimental paradigm. Following a baseline recording in which TTX was present, neurons were perfused with high KCl artificial cerebrospinal fluid (aCSF). Rat cortical neurons robustly respond to membrane depolarization, shown by the increase in ΔF/F values visualized by Ca^{2+} imaging frame images and a representative ΔF/F trace from a single experiment (Figure 3A).

We then employed the experimental paradigm presented in Figure 2 on rat cortical neurons and subsequently performed quantitative PCR (qPCR) on cDNA that was reverse transcribed from purified RNA (Table S2). The qPCR results show robust induction (~4-fold) of the IEG transcript Fos following 2 h of membrane depolarization (Figure 3B), which remains elevated at 6 h of membrane depolarization compared to

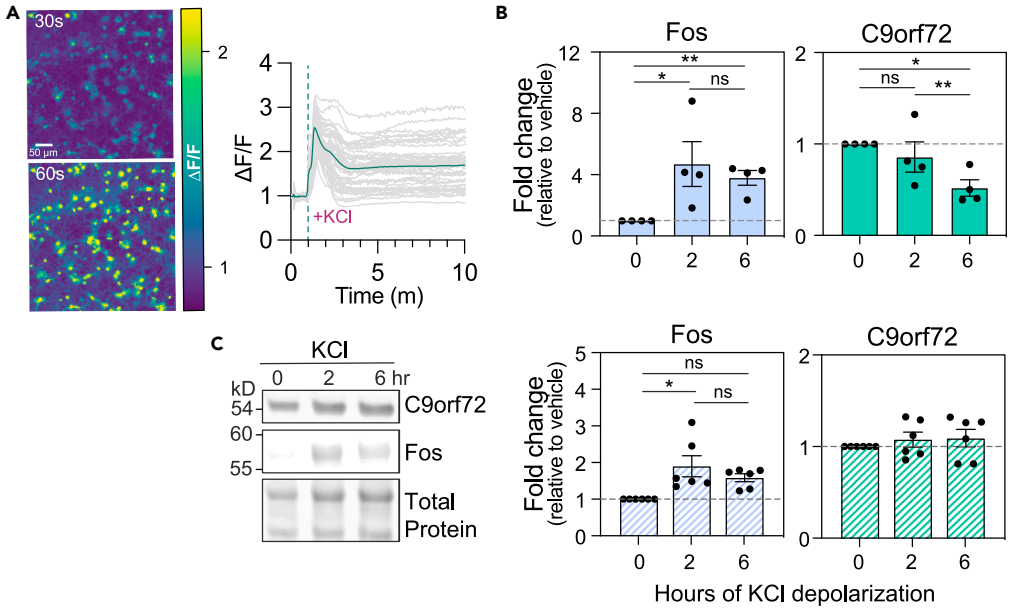

Figure 3. C9orf72 transcripts are decreased by 6 h of membrane depolarization in rodent cortical neurons

(A) Ca^{2+} imaging using the Ca^{2+} sensor Fluo-4 a.m. was performed on DIV 21 rat cortical neurons. After a baseline recording in which TTX is present, neurons were exposed to 55 mM KCl. Images of Fluo-4 a.m. loaded cortical neurons pre- and post- KCl. The scale bar indicates 10 μm. A representative ΔF/F trace indicates an increase in intracellular Ca^{2+} in response to depolarization. The gray traces are individual cells, and the dark green trace represents the mean of individual cells. The green dashed line indicates the time of stimulation. For each experiment n = 3 technical replicates with *m* = 50 cells.

(B) qPCR results showing Fos transcripts are induced rapidly following 2 h of depolarization, indicating activation of the activity-dependent transcription pathway. C9orf72 transcript levels are significantly reduced following 6 h of KCl depolarization. Technical replicates n = 4.

(C) Fos protein is increased in tandem with Fos transcripts, however, there is not a rapid reduction of C9orf72 protein levels evaluated via western blotting. Band intensity was normalized to Total Protein stain. Technical replicates n = 6.

Statistical analyses in (B) and (C) were performed by repeated measures one-way ANOVA with Tukey's multiple comparison test on dCt values for qPCR or values normalized to total protein for western blot quantification. **p < 0.01, *p < 0.05. Error bars represent the SEM.

baseline. Robust induction of IEG transcripts serve as validation of membrane depolarization and, thus, activation of the activity-dependent gene transcription pathway. We then measured total C9orf72 transcripts following membrane depolarization of rat cortical neurons. We found no significant alterations in levels of C9orf72 transcripts at 2 h but, surprisingly, we observed a significant reduction (48% decrease) in C9orf72 transcripts following 6 h of membrane depolarization (Figure 3B). We performed western blotting analyses to determine if alterations in transcript levels correlated with protein levels at these time points. Indeed, Fos protein was elevated following 2 h of depolarization, mimicking the pattern of RNA induction (Figure 3C). We did not detect the rapid changes in protein levels of C9orf72 by western blotting as observed with the transcripts, which could be in part because of protein turnover rates for this protein, which are estimated to be 6–9 h in HEK293T cells.[54] Overall, these results show that, in rat cortical neurons, C9orf72 is downregulated in response to neuronal depolarization.

Activity-dependent transcripts are induced by depolarization in human i^{3}Neurons

To determine if the activity-dependent transcriptional expression of the C9orf72 locus responds similarly in human cortical neurons as in rat primary cortical neurons, we employed membrane depolarization on several lines of human induced pluripotent stem cell (hiPSC) models. These hiPSCs, derived from several healthy individuals, termed i^{3}Neurons, contain a doxycycline-inducible Neurogenin-1 and/or Neurogenin-2 (NGN1/NGN2) cassette integrated into a safe-harbor locus site (AAVS1 or CLYBL), which quickly and robustly differentiates hiPSCs into glutamatergic cortical-like neurons after doxycycline addition (Figure 4A, Table S1).[43,44] All experiments were performed when the i^{3}Neuron lines reached full maturity (day *in vitro* 25) and were confirmed to elicit spontaneous extracellular potentials as measured

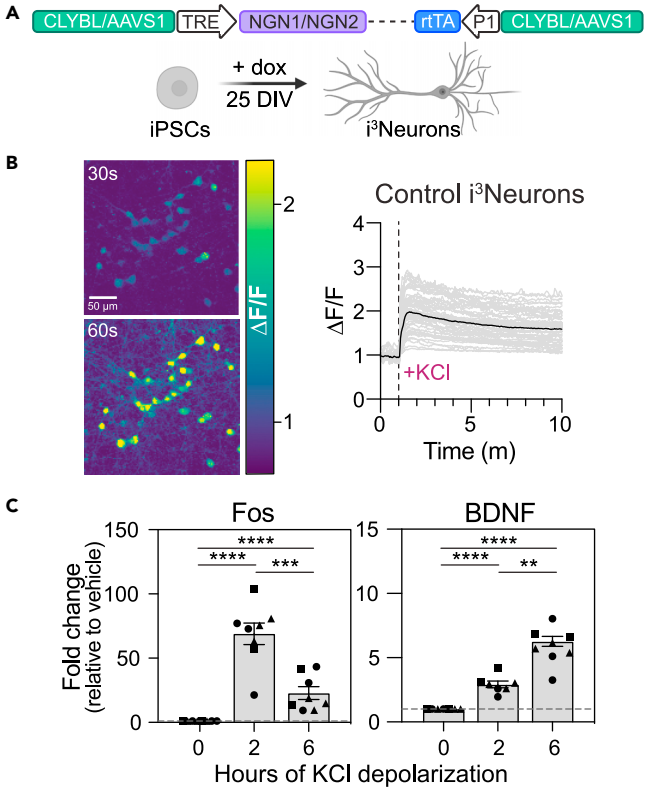

Figure 4. i^{3}Neurons robustly respond to KCl-induced membrane depolarization

(A) Schematic of approach to the generation of i^{3}Neurons. A doxycycline (dox) inducible promoter (TRE) driving the pro-neural transcription factors neurogenin-1 and/or neurogenin-2 was inserted into safe-harbor locus sites, AAVS1 or CLYBL. hiPSCs are differentiated into i^{3}Neurons following the addition of dox and are experimented upon at DIV 25.

(B) i^{3}Neurons robustly respond to membrane depolarization (55 mM KCl) via Ca^{2+} imaging using Fluo-4 a.m. Images of Fluo-4 a.m. loaded control i^{3}Neurons pre- and post- KCl. The scale bar indicates 50 µm. A representative ΔF/F trace indicates an increase in intracellular Ca^{2+} in response to depolarization. The gray traces are individual cells, and the black trace represents the mean of individual cells. For each experiment n = 3 biological replicates, *m* = 2–4 technical replicates with *o* = 50 cells.

(C) The activity-dependent transcription pathway is activated via KCl as indicated by the observed rapid induction of Fos transcripts at 2 h, and BDNF induction in the latter phase, at 6 h, measured by qPCR. For each experiment n = 3 biological replicates, *m* = 2–3 technical replicates. Each biological replicate is indicated by a unique shape. p value range ****p < 0.0001, ***p < 0.001, **p < 0.01, *p < 0.05 by repeated measures one-way ANOVA with Tukey's multiple comparison test on dCt values. Error bars represent the SEM.

by multi-electrode array (MEA) recordings (Figure S2). To first validate that these i^{3}Neurons respond robustly to the membrane depolarization experimental paradigm, we used the Ca^{2+} indicator Fluo-4 a.m. to measure the intracellular Ca^{2+} levels following KCl depolarization. As with the rat primary cortical neurons, the i^{3}Neuron cultures were silenced with TTX before exposure to KCl. Following a baseline recording in the presence of TTX, neurons were perfused with high KCl aCSF (55 mM KCl). In control i^{3}Neurons from healthy individuals, we observe a robust increase in Ca^{2+} levels that remains elevated throughout the remainder of the recording (Figure 4B). We also measured transcript levels of *bona fide* IEGs, Fos, Npas4, and LRG, brain-derived neurotrophic factor (BDNF) (Figures 4C and S3) immediately after the addition of KCl. Moreover, there was a significant induction of Fos transcripts at 2 h, which remained elevated at 6 h of depolarization compared to baseline (Figure 4C). The LRG BDNF was robustly induced at 2 h and further increased following 6 h of depolarization (Figure 4C). The induction of IEGs and LRGs at 2 h and 6 h, respectively, indicates robust activation of the activity-dependent transcription pathway in this model. Moreover, these results demonstrate that the cortical i^{3}Neuron model elicits a strong response to membrane depolarization similar to rat primary cortical neurons, and therefore is a valid and appropriate human model for investigating the relationship between neuronal depolarization and induction of transcripts.

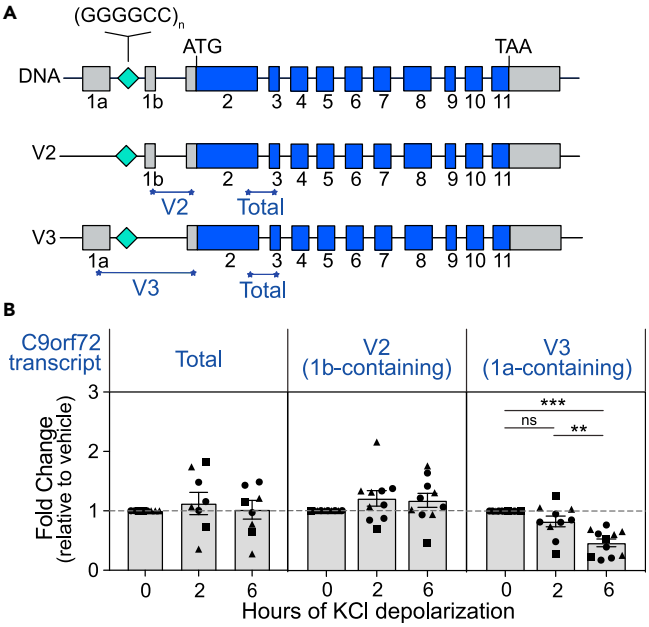

Figure 5. C9orf72 Variant 3 is reduced in control i^{3}Neurons following membrane depolarization but overall C9orf72 transcript levels are largely unchanged

(A) The C9orf72 gene is transcribed into 3 different transcript variants, Variant 1 (V1), Variant 2 (V2), and Variant 3 (V3). Consistent with other reports, V1 is not detectable in our models and is excluded from analysis and this schema. V3 utilizes an alternative first exon, exon 1a, while the predominantly expressed variant, V2 utilizes exon 1b.

(B) Levels of C9orf72 RNAs were profiled via qPCR in control i^{3}Neurons. There were no significant changes in levels of total C9orf72 transcripts over the course of depolarization. There is a slight trending increase in V2 transcript levels following depolarization. There is a significant reduction, an almost 2-fold decrease, of V3 following depolarization (a reduction of 32% and 55% at 2 and 6 h, respectively). For each experiment n = 3 biological replicates, *m* = 2–5 technical replicates. Each biological replicate is indicated by a unique shape. Statistical analyses in were performed by repeated measures one-way ANOVA with Tukey's multiple comparison test on dCt values. ***p < 0.001, **p < 0.01. Error bars represent the SEM.

C9orf72 transcript variant usage is altered following membrane depolarization in i^{3}Neurons

To determine the effect of neuronal depolarization on C9orf72 RNA levels in cortical i^{3}Neurons, we systematically profiled individual C9orf72 transcript variants transcript levels and total C9orf72 transcript levels following membrane depolarization. Three RNA transcript variants have been ubiquitously reported in the literature for C9orf72: Variant 1 (V1), which encodes a C-terminally truncated protein isoform of C9orf72; and variant 2 (V2) and variant 3 (V3), which encode full-length protein isoforms. Moreover, V1 and V3 utilize an alternative first exon, exon 1a, whereas the predominantly expressed variant, V2, utilizes exon 1b. To profile the levels of these individual C9orf72 RNA transcripts, we used commercially available and custom[2,55] Taqman qPCR assays to measure the specific C9orf72 transcript variants V2, and V3, as well as total C9orf72 using probes designed to detect scripts irrespective of the variant isoform (Figure 5A, Table S3). After performing qPCR with TaqMan assays, surprisingly, we observed a significant decrease in V3 transcripts; a reduction of 32% and 55% at 2 and 6 h, respectively. There were no significant changes in total C9orf72 transcripts or V2 transcript levels following depolarization, although V2 transcripts showed a slight trending increase over the depolarization course (Figure 5B). Consistent with other reports, V1 was below the limit of detection in these i^{3}Neurons, and therefore it was excluded from our variant analyses (data not shown).[55,56] Overall, these results demonstrate that there is a substantial shift in C9orf72 transcript variant usage following membrane depolarization in cortical-like i^{3}Neurons even though the total transcripts levels remain constant over this time course.

Membrane depolarization activates activity-dependent transcription in C9-NRE i^{3}Neurons

We then sought to determine if membrane depolarization also altered C9orf72 transcript variant usage in the context of the ALS/FTD-linked C9-NRE mutation. To do this, we employed the experimental paradigm (TTX, KCl) on several patient-derived i^{3}Neurons that carry the C9-NRE gene mutation located in the promoter region of transcript V2, or in intron 1 for V1 and V3 as shown in Figure 5A. We first determined if

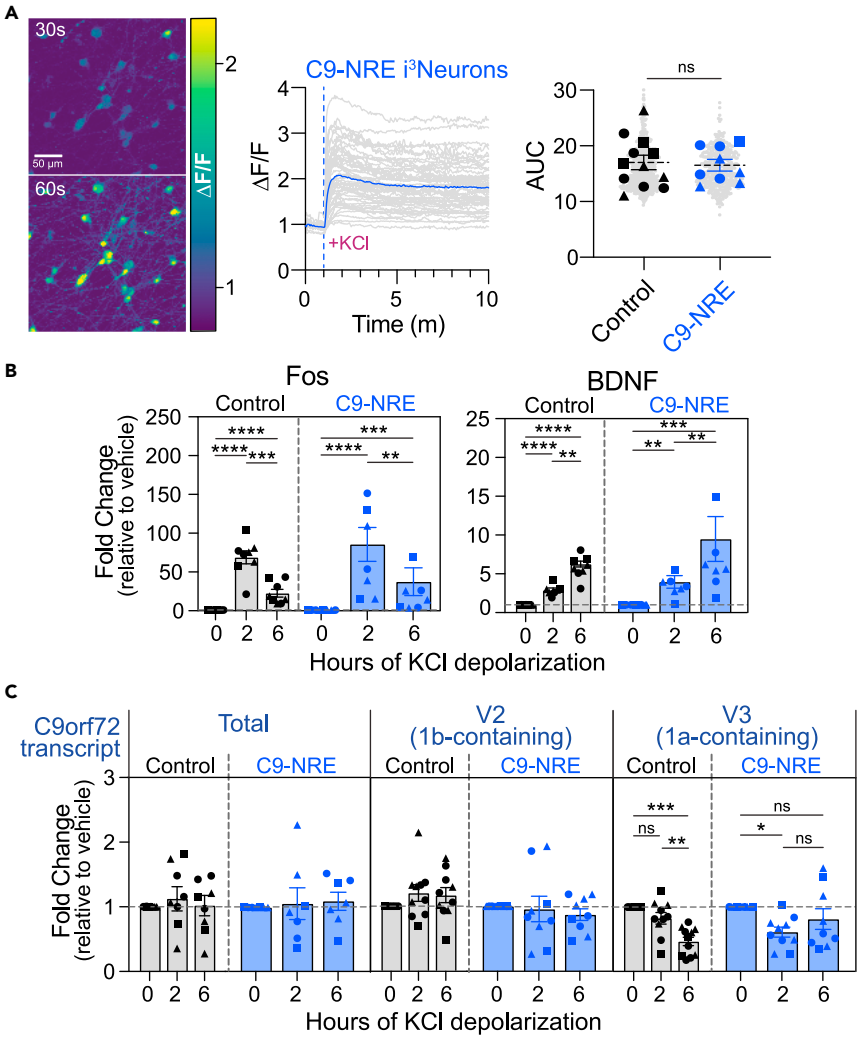

Figure 6. C9orf72 transcript levels are less altered in i^{3}Neurons from C9-NRE carriers compared to controls following membrane depolarization

(A) C9-NRE carrier-derived i^{3}Neurons robustly respond to membrane depolarization (55 mM KCl) via Ca^{2+} imaging using Fluo-4 a.m. Images of Fluo-4 a.m. loaded C9-NRE i^{3}Neurons pre- and post- KCl. The scale bar indicates 50 µm. A representative ΔF/F trace indicates an increase in intracellular Ca^{2+} in response to depolarization. The gray traces are individual cells, and the blue trace represents the mean of individual cells. The dashed blue line indicates the time of stimulation. The area under the curve (AUC) was calculated for each experiment and is represented by a SuperPlot.[68] For each experiment n = 3 biological replicates, *m* = 1–4 technical replicates with *o* = 50 cells.

(B) The activity-dependent transcription pathway is activated via KCl as indicated by the observed rapid induction of Fos transcripts at 2 h and BDNF induction in the latter phase, at 6 h, measured by qPCR. For each experiment n = 3 biological replicates, *m* = 2–3 technical replicates.

(C) Levels of C9orf72 RNAs were profiled via qPCR in C9-NRE i^{3}Neurons. There were no significant changes in levels of total C9orf72 or V2 transcripts over the course of depolarization. There is a significant reduction of V3 following 2 h depolarization (27% reduction), however, this is not to the same extent as seen in Control i^{3}Neurons. V3 levels are not significantly reduced at 6 h in C9-NRE i^{3}Neurons. For all graphs, each biological replicate is indicated by a unique shape. Statistical analyses in (A) were performed by unpaired *t*-test. Statistical analyses in (B) and (C) were performed by repeated measures one-way ANOVA with Tukey's multiple comparison test on dCt values. p value range: ****p < 0.0001, ***p < 0.001, **p < 0.01, *p < 0.05. Error bars represent the SEM.

C9-NRE i^{3}Neurons responded similarly to membrane depolarization as control i^{3}Neurons. Using the same Ca^{2+} imaging methodology previously described for control i^{3}Neurons, we indeed observe that C9-NRE i^{3}Neurons robustly respond to membrane depolarization by KCl exposure as measured by a rapidly increased influx of intracellular Ca^{2+} levels, that, like in control i^{3}Neurons, remains elevated (Figure 6A).

By quantifying the area under the curve (AUC), we determined that KCl depolarization elicits a similar response from C9-NRE and control i^{3}Neurons (Figure 6A). Following KCl depolarization, C9-NRE i^{3}Neurons also show a robust induction of activity-dependent transcripts Fos and BDNF as measured by qPCR (Figure 6B). Neither C9-NRE nor control i^{3}Neurons demonstrated KCl-induced excitotoxicity as measured by steady levels of CellTox Green, a dye that measures membrane integrity and thus serves as a proxy for cell death (Figure S4). These results indicate that, at least, some activity-dependent transcripts are induced by membrane depolarization in C9-NRE i^{3}Neurons, and, thus, may be used to study how C9orf72 responds to neuronal depolarization in a disease context.

C9orf72 transcript variant usage shows limited alteration in C9-NRE i^{3}Neurons following membrane depolarization

To determine if the C9-NRE mutation alters the transcriptional response following membrane depolarization, we measured C9orf72 RNAs in C9-ALS/FTD patient-derived i^{3}Neurons. Similar to control i^{3}Neurons, neither total C9orf72 nor V2 levels were significantly altered by membrane depolarization (Figure 6C). Strikingly, in C9-NRE i^{3}Neurons, depolarization does not result in the same reduction of V3 transcript levels as measured in the control i^{3}Neurons. The levels of V3 are slightly but significantly reduced at 2 h of depolarization in the C9-NRE i^{3}Neurons, reduction of 27% at 2 h and 23% at 6 h (Figure 6C). We then measured protein levels of Fos and C9orf72 by western blotting. As expected, we observed the induction of Fos protein following membrane depolarization and observed no differences in C9orf72 protein levels in either control or C9-NRE i^{3}Neurons at 2 h or 6 h of depolarization (Figure S5). By 12 h of recovery following depolarization, levels of V3 return to baseline and are no longer divergent from C9 total and V2 levels in Control i^{3}Neurons or C9-NRE i^{3}Neurons (Figure S6B). We observed no significant changes in C9orf72 protein levels harvested from i^{3}Neurons that were allowed to recover 6- or 12-h following depolarization (Figure S6C). These results indicate that the C9orf72 transcript variant usage following neuronal depolarization is temporally divergent in cortical-like i^{3}Neuron models from patients carrying the ALS/FTD-linked C9-NRE mutation versus healthy controls.

DISCUSSION

In this work, we show that canonical activity-dependent TFs are enriched at the promoter region of the C9orf72 gene locus in ChIP-sequencing datasets from both humans and rodents. Yet surprisingly, levels of C9orf72 RNAs were not induced on neuronal depolarization in rat cortical neurons. Rather, a significant reduction of C9orf72 transcripts was observed following 6 h of membrane depolarization. In hiPSC-derived cortical-like i^{3}Neuron models, we observe a slight increase in the most abundant C9orf72 transcript, V2. In contrast, a significant decrease in levels was observed for the V3 transcripts following 6 h of membrane depolarization. The decrease in C9orf72 V3 transcripts following 6 h of depolarization may indicate a role in the second wave of activity-dependent transcription. Of interest, total C9orf72 transcript levels remain unchanged in the control i^{3}Neurons, which suggests that this variant switching in response to depolarization may be because of a switch in transcript usage. However, in i^{3}Neurons derived from patients carrying the C9-NRE mutation, there is a temporal shift in the dynamics and magnitude of downregulation of V3 in response to depolarization, which could have important implications in neuronal-specific disease pathomechanisms for C9-NRE-linked ALS/FTD.

Activity-dependent transcription is crucial for nervous system development and homeostasis,[24,25] and our results suggest that the C9orf72 gene locus is responsive to activity-dependent changes in both rodents and human neurons. It could be reasoned that the decrease in C9orf72 transcripts in rat cortical neurons may be related to its function in regulating the lysosomal-autophagic axis. Autophagic flux and trafficking of lysosomes have emerged to be regulated by neuronal activity in some contexts.[57,58] On the other hand, it is known that C9orf72 is localized at excitatory synapses, and there is a positive correlation between C9orf72 expression and excitatory synapse number.[19] It could also be that C9orf72 is downregulated in response to neuronal activity as a means of synaptic homeostatic scaling. Much is known about transcripts that are induced on neuronal activity, but genes that are down-regulated by neuronal activity receive less focus. Several studies have investigated the activity-dependent transcriptome in hiPSC-neuron models.[59–61] However, we are the first to report the induction of early and late wave-specific activity-dependent transcripts as a result of membrane depolarization in i^{3}Neurons.

In human neurons, we do not observe changes in total C9orf72 transcripts in control i^{3}Neurons, but instead, there is a slight increase in levels of transcript V2 coupled with a significant decrease in V3 levels.

This indicates that the overall abundance of C9orf72 RNAs is not changing; instead, there is a switch in promoter/transcript usage. Of interest, the reduction in V3 transcripts following 6 h of depolarization in control i^{3}Neurons mimics the observation that C9orf72 is reduced following membrane depolarization in rodent cortical neurons. These results may indicate the potential for some level of convergent regulation of C9orf72 across species in response to neuronal activity, and perhaps a role in the second wave of activity-dependent gene regulation. These features are not recapitulated in i^{3}Neurons from patients carrying the C9-NRE mutation which, as discussed, could indicate a vital neuronal-specific disease pathomechanism. An important consideration is that the observed reduction of V3 transcripts following depolarization in the control i^{3}Neurons may be because of a decreased rate of transcription and/or changes in transcript degradation. However, this would suggest an intriguing and selective degradation mechanism specific for V3 transcripts. Some C9or7f2 transcripts have been identified as a target of nonsense-mediated decay in the context of C9-NRE-linked disease,[62] further research is needed to fully understand the mechanisms of decay for all C9or7f2 transcripts. Previous studies have shown that there is dysregulation of C9orf72 transcript variants in a disease context and that this may engender unique clinical and tissue-specific associations. In C9-NRE carrier-derived neurons, the NRE-affected C9orf72 allele preferentially uses a transcriptional start site in exon 1a (V3), upstream of the NRE, thus potentially including the NRE in mature transcripts, versus exon 1b in V2, in which the NRE is in the promoter region and proposed not to be included in mature transcripts.[63] Furthermore, previous reports show brain region-specificity in C9orf72 transcript variant expression. For example, intron 1a-containing transcripts (V1, V3) are more abundant in the frontal cortex obtained from C9-NRE carriers compared to healthy controls, whereas this effect is not seen in the cerebellum,[55] indicating the potential for neuronal subtype-specific expression patterns of transcript variants in a healthy and disease context. Our results in cortical-like i^{3}Neurons show that V3 levels (intron 1a-containing RNAs) in C9-NRE carrier i^{3}Neurons are only slightly reduced on membrane depolarization. These results suggest that the presence of the NRE alters the temporal dynamics of production or elimination of this transcript; either stabilizing transcript variants or repressing/blocking this transcriptional switch from occurring on the mutant allele. It has been proposed that intronic retention of the expanded allele, produced from either V1 or V3, is the primary source for the GOF toxicity linked to RNA-binding protein sequestration and/or DPR production.[64] Therefore, these altered dynamics may have implications on disease pathomechanisms. Future studies are necessary to evaluate the allelic-specific expression and how these transcriptional changes in response to neuronal activity may be directly relevant to cell-autonomous disease pathomechanisms.

C9orf72 protein levels are largely unaffected by the reduction of V3 post-depolarization. However, there is a slight, but insignificant, increase in protein levels that return to baseline within 6 h post-depolarization (Figure S6) in both control and C9-NRE i^{3}Neurons. The slight increase in C9orf72 protein parallels the slight increase in V2 transcripts, which could suggest that the majority of C9orf72 protein is produced from the V2 transcript. This is consistent with V2 being more abundant than V3 transcripts[55,63] and, therefore, V2 likely contributes more to overall levels of C9orf72 protein.

Cortical hyperexcitability, commonly observed early in ALS disease progression,[37,39,40] is emerging as a relevant disease modifier that has strengthened the link between neuronal activity and ALS molecular mechanisms. Our laboratory and others have shown that increased excitatory neuronal activity leads to elevated levels of di-peptide repeat proteins (DPRs) in human and rodent neurons.[41,42] It is important to note that it is difficult to dissect the source of increased levels of DPRs; it could be because of increased transcripts which serve as a template of RAN translation, and/or it could be because of increased occurrence of RAN translation. Another notable ALS-related protein that has emerged to be regulated by neuronal activity is the nuclear protein TAR DNA-binding protein 43 (TDP-43). Cytoplasmic accumulation of TDP-43 is a pathological hallmark of ALS is proteinaceous TDP-43 inclusions,[65] and neuronal hyperactivity leads to the upregulation of a truncated isoform of TDP-43 which then leads to nuclear clearance and cytoplasmic aggregation of full-length TDP-43, recapitulating disease hallmarks.[43] Furthermore, dysregulation of activity-dependent transcription factors such as CREB and the AP-1 transcription factor complex have been reported in C9-NRE hiPSC neuronal models.[42,66] Although mimicking a hyper-excitable state may be important in untangling activity-dependent pathomechanisms in ALS and FTD, it is important to note that the mode of stimulation used in this current study, membrane depolarization by KCl, does not recapitulate hyperexcitability. Instead, the use of our experimental paradigm allows reliable activation of the activity-dependent transcription factor pathway by prolonged depolarization,[24,48,49,67] in which we

have investigated the role of C9orf72 RNAs. In this present work, we have demonstrated that ubiquitous markers of neuronal activity (Fos, BDNF) are indeed induced in C9-NRE i^{3}Neurons following membrane depolarization, indicating the proper function of the activity-dependent transcription pathway on some level, albeit with limited evidence for temporal differences in response to this activity. Given the increasing evidence for dysregulation of neuronal activity-dependent programs, we speculate that sustained neuronal depolarization could also induce a widespread divergent transcriptional response in C9-NRE i^{3}Neurons, which requires future studies.

Limitations of the study

There is a slight discrepancy in the amount of total C9orf72 transcripts measured in the C9-NRE i^{3}Neurons versus the summation of individual canonical C9orf72 transcripts. This difference may be attributed to the presence of noncanonical transcript variants, which we did not identify in our study. To address this limitation, future research incorporating advanced techniques, like long-read sequencing, will be necessary to identify all noncanonical C9orf72 transcripts and investigate their modulation in response to neuronal depolarization. It is worth noting that we were unable to differentiate between transcripts originating from the NRE-affected allele. Long-read sequencing can provide a solution to this issue as well. Additional studies are needed to elucidate the allele-specific regulation of C9orf72 transcripts under conditions of neuronal depolarization.

STAR★METHODS

Detailed methods are provided in the online version of this paper and include the following:

- KEY RESOURCES TABLE
- RESOURCE AVAILABILITY
  - Lead contact
  - Materials availability
  - Data and code availability
- EXPERIMENTAL MODEL DETAILS
  - hiPSC culturing and i^{3}Neuron differentiation
  - Primary rat cortical cultures
- METHOD DETAILS
  - KCl depolarization of neurons
  - Calcium imaging
  - Quantitative polymerase chain reaction (qPCR)
  - Western blotting
  - Survival assay
  - Multi-electrode Array (MEA)
- QUANTIFICATION AND STATISTICAL ANALYSIS

SUPPLEMENTAL INFORMATION

Supplemental information can be found online at https://doi.org/10.1016/j.isci.2023.106959.

ACKNOWLEDGMENTS

We would like to thank the Jefferson Weinberg ALS Center members for providing valuable feedback on this manuscript. We would also like to acknowledge Sami Barmada and Michael Ward for generously gifting us with i^{3}Neuron lines. Additional figures were created with BioRender.com. This work was supported by the following sources: the National Institutes of Health grants RF1NS114128 and R21NS116761 to A.R.H.; and R21-NS090912 and RF1-AG057882 to D.T. Additional support provided by the Family Strong for ALS and the Farber Family Foundation to A.R.H. and D.T.

AUTHOR CONTRIBUTIONS

L.T.G. and A.R.H. conceptualized the research. L.T.G. designed all experiments with input from A.R.H. and D.T. L.T.G. performed all experiments and all data analyses and was overseen by A.R.H. and D.T. L.T.G. led the manuscript writing with A.R.H. L.T.G. and A.R.H. developed and assembled the figures. All authors read and approved the final manuscript.

DECLARATION OF INTERESTS

The authors declare no conflicts of interest.

Received: January 24, 2023
Revised: April 19, 2023
Accepted: May 22, 2023
Published: May 24, 2023

REFERENCES

1. Renton, A.E., Majounie, E., Waite, A., Simón-Sánchez, J., Rollinson, S., Gibbs, J.R., Schymick, J.C., Laaksovirta, H., van Swieten, J.C., Myllykangas, L., et al. (2011). A hexanucleotide repeat expansion in C9ORF72 is the cause of chromosome 9p21-linked ALS-FTD. Neuron *72*, 257–268. https://doi.org/10.1016/j.neuron.2011.09.010.

2. DeJesus-Hernandez, M., Mackenzie, I.R., Boeve, B.F., Boxer, A.L., Baker, M., Rutherford, N.J., Nicholson, A.M., Finch, N.A., Flynn, H., Adamson, J., et al. (2011). Expanded GGGGCC hexanucleotide repeat in noncoding region of C9ORF72 causes chromosome 9p-linked FTD and ALS. Neuron *72*, 245–256. https://doi.org/10.1016/j.neuron.2011.09.011.

3. Mori, K., Lammich, S., Mackenzie, I.R.A., Forné, I., Zilow, S., Kretzschmar, H., Edbauer, D., Janssens, J., Kleinberger, G., Cruts, M., et al. (2013). hnRNP A3 binds to GGGGCC repeats and is a constituent of p62-positive/TDP43-negative inclusions in the hippocampus of patients with C9orf72 mutations. Acta Neuropathol. *125*, 413–423. https://doi.org/10.1007/s00401-013-1088-7.

4. Donnelly, C.J., Zhang, P.W., Pham, J.T., Haeusler, A.R., Mistry, N.A., Vidensky, S., Daley, E.L., Poth, E.M., Hoover, B., Fines, D.M., et al. (2013). RNA toxicity from the ALS/FTD C9ORF72 expansion is mitigated by antisense intervention. Neuron *80*, 415–428. https://doi.org/10.1016/j.neuron.2013.10.015.

5. Haeusler, A.R., Donnelly, C.J., Periz, G., Simko, E.A.J., Shaw, P.G., Kim, M.S., Maragakis, N.J., Troncoso, J.C., Pandey, A., Sattler, R., et al. (2014). C9orf72 nucleotide repeat structures initiate molecular cascades of disease. Nature *507*, 195–200. https://doi.org/10.1038/nature13124.

6. Burguete, A.S., Almeida, S., Gao, F.B., Kalb, R., Akins, M.R., and Bonini, N.M. (2015). GGGGCC microsatellite RNA is neuritically localized, induces branching defects, and perturbs transport granule function. Elife *4*, e08881. https://doi.org/10.7554/eLife.08881.

7. Conlon, E.G., Lu, L., Sharma, A., Yamazaki, T., Tang, T., Shneider, N.A., and Manley, J.L. (2016). The C9ORF72 GGGGCC expansion forms RNA G-quadruplex inclusions and sequesters hnRNP H to disrupt splicing in ALS brains. Elife *5*, e17820. https://doi.org/10.7554/eLife.17820.

8. Balendra, R., and Isaacs, A.M. (2018). C9orf72-mediated ALS and FTD: multiple pathways to disease. Nat. Rev. Neurol. *14*, 544–558. https://doi.org/10.1038/s41582-018-0047-2.

9. Wen, X., Tan, W., Westergard, T., Krishnamurthy, K., Markandaiah, S.S., Shi, Y., Lin, S., Shneider, N.A., Monaghan, J., Pandey, U.B., et al. (2014). Antisense proline-arginine RAN dipeptides linked to C9ORF72-ALS/FTD form toxic nuclear aggregates that initiate in vitro and in vivo neuronal death. Neuron *84*, 1213–1225. https://doi.org/10.1016/j.neuron.2014.12.010.

10. Wen, X., Westergard, T., Pasinelli, P., and Trotti, D. (2017). Pathogenic determinants and mechanisms of ALS/FTD linked to hexanucleotide repeat expansions in the C9orf72 gene. Neurosci. Lett. *636*, 16–26. https://doi.org/10.1016/j.neulet.2016.09.007.

11. Shi, Y., Lin, S., Staats, K.A., Li, Y., Chang, W.H., Hung, S.T., Hendricks, E., Linares, G.R., Wang, Y., Son, E.Y., et al. (2018). Haploinsufficiency leads to neurodegeneration in C9ORF72 ALS/FTD human induced motor neurons. Nat. Med. *24*, 313–325. https://doi.org/10.1038/nm.4490.

12. O'Rourke, J.G., Bogdanik, L., Yáñez, A., Lall, D., Wolf, A.J., Muhammad, A.K., Ho, R., Carmona, S., Vit, J.P., Zarrow, J., et al. (2016). C9orf72 is required for proper macrophage and microglial function in mice. Science *351*, 1324–1329. https://doi.org/10.1126/science.aaf1064.

13. Burberry, A., Suzuki, N., Wang, J.Y., Moccia, R., Mordes, D.A., Stewart, M.H., Suzuki-Uematsu, S., Ghosh, S., Singh, A., Merkle, F.T., et al. (2016). Loss-of-function mutations in the C9ORF72 mouse ortholog cause fatal autoimmune disease. Sci. Transl. Med. *8*, 347ra93. https://doi.org/10.1126/scitranslmed.aaf6038.

14. McCauley, M.E., O'Rourke, J.G., Yáñez, A., Markman, J.L., Ho, R., Wang, X., Chen, S., Lall, D., Jin, M., Muhammad, A.K., et al. (2020). C9orf72 in myeloid cells suppresses STING-induced inflammation. Nature *585*, 96–101. https://doi.org/10.1038/s41586-020-2625-x.

15. Amick, J., Roczniak-Ferguson, A., and Ferguson, S.M. (2016). C9orf72 binds SMCR8, localizes to lysosomes, and regulates mTORC1 signaling. Mol. Biol. Cell *27*, 3040–3051. https://doi.org/10.1091/mbc.E16-01-0003.

16. Frick, P., Sellier, C., Mackenzie, I.R.A., Cheng, C.Y., Tahraoui-Bories, J., Martinat, C., Pasterkamp, R.J., Prudlo, J., Edbauer, D., Oulad-Abdelghani, M., et al. (2018). Novel antibodies reveal presynaptic localization of C9orf72 protein and reduced protein levels in C9orf72 mutation carriers. Acta Neuropathol. Commun. *6*, 72. https://doi.org/10.1186/s40478-018-0579-0.

17. Atkinson, R.A.K., Fernandez-Martos, C.M., Atkin, J.D., Vickers, J.C., and King, A.E. (2015). C9ORF72 expression and cellular localization over mouse development. Acta Neuropathol. Commun. *3*, 59. https://doi.org/10.1186/s40478-015-0238-7.

18. Xiao, S., McKeever, P.M., Lau, A., and Robertson, J. (2019). Synaptic localization of C9orf72 regulates post-synaptic glutamate receptor 1 levels. Acta Neuropathol. Commun. *7*, 161. https://doi.org/10.1186/s40478-019-0812-5.

19. Bauer, C.S., Cohen, R.N., Sironi, F., Livesey, M.R., Gillingwater, T.H., Highley, J.R., Fillingham, D.J., Coldicott, I., Smith, E.F., Gibson, Y.B., et al. (2022). An interaction between synapsin and C9orf72 regulates excitatory synapses and is impaired in ALS/FTD. Acta Neuropathol. *144*, 437–464. https://doi.org/10.1007/s00401-022-02470-z.

20. Iyer, S., Subramanian, V., and Acharya, K.R. (2018). C9orf72, a protein associated with amyotrophic lateral sclerosis (ALS) is a guanine nucleotide exchange factor. PeerJ *6*, e5815. https://doi.org/10.7717/peerj.5815.

21. Tang, B.L. (2016). C9orf72's interaction with rab GTPases-modulation of membrane traffic and autophagy. Front. Cell. Neurosci. *10*, 228. https://doi.org/10.3389/fncel.2016.00228.

22. Lall, D., Lorenzini, I., Mota, T.A., Bell, S., Mahan, T.E., Ulrich, J.D., Davtyan, H., Rexach, J.E., Muhammad, A.K., Shelest, O., et al. (2021). C9orf72 deficiency promotes microglial-mediated synaptic loss in aging and amyloid accumulation. Neuron *109*, 2275–2291.e8. https://doi.org/10.1016/j.neuron.2021.05.020.

23. Iyer, S., Acharya, K.R., and Subramanian, V. (2018). A comparative bioinformatic analysis of C9orf72. PeerJ *6*, e4391. https://doi.org/10.7717/peerj.4391.

24. Yap, E.L., and Greenberg, M.E. (2018). Activity-regulated transcription: bridging the gap between neural activity and behavior. Neuron *100*, 330–348. https://doi.org/10.1016/j.neuron.2018.10.013.

25. Benito, E., and Barco, A. (2015). The neuronal activity-driven transcriptome. Mol. Neurobiol. *51*, 1071–1088. https://doi.org/10.1007/s12035-014-8772-z.

26. Lepeta, K., Lourenco, M.V., Schweitzer, B.C., Martino Adami, P.V., Banerjee, P., Catuara-

Solarz, S., de La Fuente Revenga, M., Guillem, A.M., Haidar, M., Ijomone, O.M., et al. (2016). Synaptopathies: synaptic dysfunction in neurological disorders - a review from students to students. J. Neurochem. *138*, 785–805. https://doi.org/10.1111/jnc.13713.

27. Ghaffari, L.T., Trotti, D., Haeusler, A.R., and Jensen, B.K. (2022). Breakdown of the central synapses in C9orf72-linked ALS/FTD. Front. Mol. Neurosci. *15*, 1005112. https://doi.org/10.3389/fnmol.2022.1005112.

28. Tyssowski, K.M., DeStefino, N.R., Cho, J.H., Dunn, C.J., Poston, R.G., Carty, C.E., Jones, R.D., Chang, S.M., Romeo, P., Wurzelmann, M.K., et al. (2018). Different neuronal activity patterns induce different gene expression programs. Neuron *98*, 530–546.e11. https://doi.org/10.1016/j.neuron.2018.04.001.

29. Su, Y., Shin, J., Zhong, C., Wang, S., Roychowdhury, P., Lim, J., Kim, D., Ming, G.L., and Song, H. (2017). Neuronal activity modifies the chromatin accessibility landscape in the adult brain. Nat. Neurosci. *20*, 476–483. https://doi.org/10.1038/nn.4494.

30. Bayraktar, G., Yuanxiang, P., Confettura, A.D., Gomes, G.M., Raza, S.A., Stork, O., Tajima, S., Suetake, I., Karpova, A., Yildirim, F., and Kreutz, M.R. (2020). Synaptic control of DNA methylation involves activity-dependent degradation of DNMT3A1 in the nucleus. Neuropsychopharmacology *45*, 2120–2130. https://doi.org/10.1038/s41386-020-0780-2.

31. Guo, J.U., Ma, D.K., Mo, H., Ball, M.P., Jang, M.H., Bonaguidi, M.A., Balazer, J.A., Eaves, H.L., Xie, B., Ford, E., et al. (2011). Neuronal activity modifies the DNA methylation landscape in the adult brain. Nat. Neurosci. *14*, 1345–1351. https://doi.org/10.1038/nn.2900.

32. Ju, W., Morishita, W., Tsui, J., Gaietta, G., Deerinck, T.J., Adams, S.R., Garner, C.C., Tsien, R.Y., Ellisman, M.H., and Malenka, R.C. (2004). Activity-dependent regulation of dendritic synthesis and trafficking of AMPA receptors. Nat. Neurosci. *7*, 244–253. https://doi.org/10.1038/nn1189.

33. Voigt, T., Baier, H., and Dolabela de Lima, A. (1997). Synchronization of neuronal activity promotes survival of individual rat neocortical neurons in early development. Eur. J. Neurosci. *9*, 990–999. https://doi.org/10.1111/j.1460-9568.1997.tb01449.x.

34. Chopra, R., and Shakkottai, V.G. (2014). The role for alterations in neuronal activity in the pathogenesis of polyglutamine repeat disorders. Neurotherapeutics *11*, 751–763. https://doi.org/10.1007/s13311-014-0289-7.

35. Geevasinga, N., Menon, P., Nicholson, G.A., Ng, K., Howells, J., Kril, J.J., Yiannikas, C., Kiernan, M.C., and Vucic, S. (2015). Cortical function in asymptomatic carriers and patients with C9orf72 amyotrophic lateral sclerosis. JAMA Neurol. *72*, 1268–1274. https://doi.org/10.1001/jamaneurol.2015.1872.

36. Geevasinga, N., Menon, P., Özdinler, P.H., Kiernan, M.C., and Vucic, S. (2016). Pathophysiological and diagnostic implications of cortical dysfunction in ALS. Nat. Rev. Neurol. *12*, 651–661. https://doi.org/10.1038/nrneurol.2016.140.

37. Schanz, O., Bageac, D., Braun, L., Traynor, B.J., Lehky, T.J., and Floeter, M.K. (2016). Cortical hyperexcitability in patients with C9ORF72 mutations: relationship to phenotype. Muscle Nerve *54*, 264–269. https://doi.org/10.1002/mus.25047.

38. Vucic, S., and Kiernan, M.C. (2006). Novel threshold tracking techniques suggest that cortical hyperexcitability is an early feature of motor neuron disease. Brain *129*, 2436–2446. https://doi.org/10.1093/brain/awl172.

39. Vucic, S., Nicholson, G.A., and Kiernan, M.C. (2008). Cortical hyperexcitability may precede the onset of familial amyotrophic lateral sclerosis. Brain *131*, 1540–1550. https://doi.org/10.1093/brain/awn071.

40. Wainger, B.J., and Cudkowicz, M.E. (2015). Cortical hyperexcitability in amyotrophic lateral sclerosis: C9orf72 repeats. JAMA Neurol. *72*, 1235–1236. https://doi.org/10.1001/jamaneurol.2015.2197.

41. Westergard, T., McAvoy, K., Russell, K., Wen, X., Pang, Y., Morris, B., Pasinelli, P., Trotti, D., and Haeusler, A. (2019). Repeat-associated non-AUG translation in C9orf72-ALS/FTD is driven by neuronal excitation and stress. EMBO Mol. Med. *11*, e9423. https://doi.org/10.15252/emmm.201809423.

42. Catanese, A., Rajkumar, S., Sommer, D., Freisem, D., Wirth, A., Aly, A., Massa-López, D., Olivieri, A., Torelli, F., Ioannidis, V., et al. (2021). Synaptic disruption and CREB-regulated transcription are restored by K(+) channel blockers in ALS. EMBO Mol. Med. *13*, e13131. https://doi.org/10.15252/emmm.202013131.

43. Weskamp, K., Tank, E.M., Miguez, R., McBride, J.P., Gómez, N.B., White, M., Lin, Z., Gonzalez, C.M., Serio, A., Sreedharan, J., and Barmada, S.J. (2020). Shortened TDP43 isoforms upregulated by neuronal hyperactivity drive TDP43 pathology in ALS. J. Clin. Invest. *130*, 1139–1155. https://doi.org/10.1172/JCI130988.

44. Fernandopulle, M.S., Prestil, R., Grunseich, C., Wang, C., Gan, L., and Ward, M.E. (2018). Transcription factor-mediated differentiation of human iPSCs into neurons. Curr. Protoc. Cell Biol. *79*, e51. https://doi.org/10.1002/cpcb.51.

45. Luo, Y., Hitz, B.C., Gabdank, I., Hilton, J.A., Kagda, M.S., Lam, B., Myers, Z., Sud, P., Jou, J., Lin, K., et al. (2020). New developments on the Encyclopedia of DNA Elements (ENCODE) data portal. Nucleic Acids Res. *48*, D882–D889. https://doi.org/10.1093/nar/gkz1062.

46. ENCODE Project Consortium (2012). An integrated encyclopedia of DNA elements in the human genome. Nature *489*, 57–74. https://doi.org/10.1038/nature11247.

47. Hammal, F., de Langen, P., Bergon, A., Lopez, F., and Ballester, B. (2022). ReMap 2022: a database of Human, Mouse, Drosophila and Arabidopsis regulatory regions from an integrative analysis of DNA-binding sequencing experiments. Nucleic Acids Res. *50*, D316–D325. https://doi.org/10.1093/nar/gkab996.

48. Rienecker, K.D.A., Poston, R.G., and Saha, R.N. (2020). Merits and limitations of studying neuronal depolarization-dependent processes using elevated external potassium. ASN Neuro *12*. 1759091420974807. https://doi.org/10.1177/1759091420974807.

49. Kim, T.K., Hemberg, M., Gray, J.M., Costa, A.M., Bear, D.M., Wu, J., Harmin, D.A., Laptewicz, M., Barbara-Haley, K., Kuersten, S., et al. (2010). Widespread transcription at neuronal activity-regulated enhancers. Nature *465*, 182–187. https://doi.org/10.1038/nature09033.

50. Bading, H., Ginty, D.D., and Greenberg, M.E. (1993). Regulation of gene expression in hippocampal neurons by distinct calcium signaling pathways. Science *260*, 181–186. https://doi.org/10.1126/science.8097060.

51. Ghosh, A., and Greenberg, M.E. (1995). Calcium signaling in neurons: molecular mechanisms and cellular consequences. Science *268*, 239–247. https://doi.org/10.1126/science.7716515.

52. Groth, R.D., Dunbar, R.L., and Mermelstein, P.G. (2003). Calcineurin regulation of neuronal plasticity. Biochem. Biophys. Res. Commun. *311*, 1159–1171. https://doi.org/10.1016/j.bbrc.2003.09.002.

53. Kingsbury, T.J., Bambrick, L.L., Roby, C.D., and Krueger, B.K. (2007). Calcineurin activity is required for depolarization-induced, CREB-dependent gene transcription in cortical neurons. J. Neurochem. *103*, 761–770. https://doi.org/10.1111/j.1471-4159.2007.04801.x.

54. Ugolino, J., Ji, Y.J., Conchina, K., Chu, J., Nirujogi, R.S., Pandey, A., Brady, N.R., Hamacher-Brady, A., and Wang, J. (2016). Loss of C9orf72 enhances autophagic activity via deregulated mTOR and TFEB signaling. PLoS Genet. *12*, e1006443. https://doi.org/10.1371/journal.pgen.1006443.

55. van Blitterswijk, M., Gendron, T.F., Baker, M.C., DeJesus-Hernandez, M., Finch, N.A., Brown, P.H., Daughrity, L.M., Murray, M.E., Heckman, M.G., Jiang, J., et al. (2015). Novel clinical associations with specific C9ORF72 transcripts in patients with repeat expansions in C9ORF72. Acta Neuropathol. *130*, 863–876. https://doi.org/10.1007/s00401-015-1480-6.

56. Ebbert, M.T.W., Ross, C.A., Pregent, L.J., Lank, R.J., Zhang, C., Katzman, R.B., Jansen-West, K., Song, Y., da Rocha, E.L., Palmucci, C., et al. (2017). Conserved DNA methylation combined with differential frontal cortex and cerebellar expression distinguishes C9orf72-associated and sporadic ALS, and implicates SERPINA1 in disease. Acta Neuropathol. *134*, 715–728. https://doi.org/10.1007/s00401-017-1760-4.

57. Shehata, M., Matsumura, H., Okubo-Suzuki, R., Ohkawa, N., and Inokuchi, K. (2012). Neuronal stimulation induces autophagy in hippocampal neurons that is involved in

AMPA receptor degradation after chemical long-term depression. J. Neurosci. *32*, 10413–10422. https://doi.org/10.1523/JNEUROSCI.4533-11.2012.

58. Goo, M.S., Sancho, L., Slepak, N., Boassa, D., Deerinck, T.J., Ellisman, M.H., Bloodgood, B.L., and Patrick, G.N. (2017). Activity-dependent trafficking of lysosomes in dendrites and dendritic spines. J. Cell Biol. *216*, 2499–2513. https://doi.org/10.1083/jcb.201704068.

59. Qiu, J., McQueen, J., Bilican, B., Dando, O., Magnani, D., Punovuori, K., Selvaraj, B.T., Livesey, M., Haghi, G., Heron, S., et al. (2016). Evidence for evolutionary divergence of activity-dependent gene expression in developing neurons. Elife *5*, e20337. https://doi.org/10.7554/eLife.20337.

60. Ataman, B., Boulting, G.L., Harmin, D.A., Yang, M.G., Baker-Salisbury, M., Yap, E.L., Malik, A.N., Mei, K., Rubin, A.A., Spiegel, I., et al. (2016). Evolution of Osteocrin as an activity-regulated factor in the primate brain. Nature *539*, 242–247. https://doi.org/10.1038/nature20111.

61. Pruunsild, P., Bengtson, C.P., and Bading, H. (2017). Networks of cultured iPSC-derived neurons reveal the human synaptic activity-regulated adaptive gene program. Cell Rep. *18*, 122–135. https://doi.org/10.1016/j.celrep.2016.12.018.

62. Ortega, J.A., Daley, E.L., Kour, S., Samani, M., Tellez, L., Smith, H.S., Hall, E.A., Esengul, Y.T., Tsai, Y.H., Gendron, T.F., et al. (2020). Nucleocytoplasmic proteomic analysis uncovers eRF1 and nonsense-mediated decay as modifiers of ALS/FTD C9orf72 toxicity. Neuron *106*, 90–107.e13. https://doi.org/10.1016/j.neuron.2020.01.020.

63. Sareen, D., O'Rourke, J.G., Meera, P., Muhammad, A.K., Grant, S., Simpkinson, M., Bell, S., Carmona, S., Ornelas, L., Sahabian, A., et al. (2013). Targeting RNA foci in iPSC-derived motor neurons from ALS patients with a C9ORF72 repeat expansion. Sci. Transl. Med. *5*, 208ra149. https://doi.org/10.1126/scitranslmed.3007529.

64. Wang, S., Latallo, M.J., Zhang, Z., Huang, B., Bobrovnikov, D.G., Dong, D., Livingston, N.M., Tjoeng, W., Hayes, L.R., Rothstein, J.D., et al. (2021). Nuclear export and translation of circular repeat-containing intronic RNA in C9ORF72-ALS/FTD. Nat. Commun. *12*, 4908. https://doi.org/10.1038/s41467-021-25082-9.

65. Chen-Plotkin, A.S., Lee, V.M.Y., and Trojanowski, J.Q. (2010). TAR DNA-binding protein 43 in neurodegenerative disease. Nat. Rev. Neurol. *6*, 211–220. https://doi.org/10.1038/nrneurol.2010.18.

66. Li, J., Lim, R.G., Kaye, J.A., Dardov, V., Coyne, A.N., Wu, J., Milani, P., Cheng, A., Thompson, T.G., Ornelas, L., et al. (2021). NeuroLINCS Consortium. An integrated multi-omic analysis of iPSC-derived motor neurons from C9ORF72 ALS patients. iScience *24*, 103221. https://doi.org/10.1016/j.isci.2021.103221.

67. Malik, A.N., Vierbuchen, T., Hemberg, M., Rubin, A.A., Ling, E., Couch, C.H., Stroud, H., Spiegel, I., Farh, K.K.H., Harmin, D.A., and Greenberg, M.E. (2014). Genome-wide identification and characterization of functional neuronal activity-dependent enhancers. Nat. Neurosci. *17*, 1330–1339. https://doi.org/10.1038/nn.3808.

68. Lord, S.J., Velle, K.B., Mullins, R.D., and Fritz-Laylin, L.K. (2020). SuperPlots: communicating reproducibility and variability in cell biology. J. Cell Biol. *219*, e202001064. https://doi.org/10.1083/jcb.202001064.

69. Laflamme, C., McKeever, P.M., Kumar, R., Schwartz, J., Kolahdouzan, M., Chen, C.X., You, Z., Benaliouad, F., Gileadi, O., McBride, H.M., et al. (2019). Implementation of an antibody characterization procedure and application to the major ALS/FTD disease gene C9ORF72. Elife *8*, e48363. https://doi.org/10.7554/eLife.48363.

STAR★METHODS

KEY RESOURCES TABLE

REAGENT or RESOURCE	SOURCE	IDENTIFIER
Antibodies		
Anti-C9orf72	GeneTex	clone GT779 Cat # GTX632041; RRID: AB_2784546
Anti-C9orf72	GeneTex	clone GT1553 Cat # GTX634482; RRID: AB_2784545
Anti-c-Fos	Cell Signaling	clone 9F6 Cat # 2250T; RRID: AB_2247211
Goat anti-Mouse IgG (H+L) Highly Cross-Adsorbed Secondary Antibody, Alexa Fluor Plus 800	Fisher Scientific	Cat # A32730; RRID: AB_2633279
Goat anti-Rabbit IgG (H+L) Highly Cross-Adsorbed Secondary Antibody, Alexa Fluor Plus 680	Fisher Scientific	Cat # A32734; RRID: AB_2633283
Chemicals, peptides, and recombinant proteins		
Essential 8™ Medium	Gibco	A1517001
Matrigel™ hESC-Qualified Matrix	Corning	354277
DMEM/F12 1:1 medium with L-glutamine, HEPES	Cytiva	SH30023.01
N-2 Supplement (100X)	Gibco	17502048
MEM Non-Essential Amino Acids Solution (100X)	Gibco	11140050
GlutaMAX™ Supplement	Gibco	35050061
Doxycycline	Sigma-Aldrich	D9891
Poly-L-ornithine hydrobromide,mol wt 30,000-70,000	Sigma-Aldrich	P3655
BrainPhys™ Neuronal Medium	STEMCELL Technologies	05790
Recombinant Human/Murine/Rat BDNF	PeproTech	450-02
Recombinant Human NT-3	PeproTech	450-03
Laminin Mouse Protein, Natural	Gibco	23017015
Tetrodotoxin citrate	Tocris	1069
B27 Supplement (50x)	Gibco	17504044
Fluo-4 AM	Invitrogen	F14201
Poly-D-lysine hydrobromide	Sigma-Aldrich	P0899
Neurobasal™ Medium	Gibco	21103049
PowerUp™ SYBR™ Green Master Mix	Thermo Fisher	A25742
QuantiTect Reverse Transcription Kit	Qiagen	205311
RNeasy Plus Mini Kit	Qiagen	74136
Matrigel™ hESC-Qualified Matrix	Corning	354277
DMEM/F12 1:1 medium with L-glutamine, HEPES	Cytiva	SH30023.01
N-2 Supplement (100X)	Gibco	17502048
MEM Non-Essential Amino Acids Solution (100X)	Gibco	11140050
GlutaMAX™ Supplement	Gibco	35050061
Doxycycline	Sigma-Aldrich	D9891

(*Continued on next page*)

Continued

REAGENT or RESOURCE	SOURCE	IDENTIFIER
Poly-L-ornithine hydrobromide,mol wt 30,000-70,000	Sigma-Aldrich	P3655
BrainPhys™ Neuronal Medium	STEMCELL Technologies	05790
Recombinant Human/Murine/Rat BDNF	PeproTech	450-02
Recombinant Human NT-3	PeproTech	450-03
Laminin Mouse Protein, Natural	Gibco	23017015
Tetrodotoxin citrate	Tocris	1069
B27 Supplement (50x)	Gibco	17504044
Fluo-4 AM	Invitrogen	F14201
Poly-D-lysine hydrobromide	Sigma-Aldrich	P0899
Neurobasal™ Medium	Gibco	21103049
PowerUp™ SYBR™ Green Master Mix	Thermo Fisher	A25742
QuantiTect Reverse Transcription Kit	Qiagen	205311
RNeasy Plus Mini Kit	Qiagen	74136
Critical commercial assays		
CellTox™ Green Cytotoxicity Assay	Promega	G8741
CytoView MEA plate	Axion Biosystems	M384-tMEA-24W
CytoView MEA plate	Axion Biosystems	M384-tMEA-24W
Deposited data		
ENCODE Project ChIP-seq	UCSC Genome Browser	https://www.encodeproject.org/
ReMAP Atlas of Regulatory Regions	UCSC Genome Browser	https://remap.univ-amu.fr/
Experimental models: cell lines		
iPSC-i^{3}Neuron lines	See Table S1	
Oligonucleotides		
qPCR primers (See Table S2)	This paper	N/A
Taqman Assays (See Table S3).	Life Technologies	N/A
Taqman Assays (See Table S3).	Life Technologies	N/A
Software and algorithms		
NIS Elements Software	Nikon	https://www.microscope.healthcare.nikon.com/products/software/nis-elements
Prism 9	GraphPad	https://www.graphpad.com/
QuantStudio Design & Analysis	ThermoFisher Scientific	https://www.thermofisher.com/us/en/home/digital-science/thermo-fisher-connect.html
Image Studio 5.2.5	Li-Cor	https://www.licor.com/bio/image-studio/

RESOURCE AVAILABILITY

Lead contact

Requests for resources and reagents should be directed to the lead contact, Aaron Haeusler (aaron.haeusler@jefferson.edu).

Materials availability

This study did not generate new unique reagents.

Data and code availability

- Data reported in this publication will be shared upon request from the lead contact.
- This study did not generate unique code.

- Any additional information required to reanalyze the data reported in this paper is available from the lead contact upon request.

EXPERIMENTAL MODEL DETAILS

hiPSC culturing and i^{3}Neuron differentiation

hiPSC-i^{3}Neuron lines were generously gifted by Dr. Sami Barmada (University of Michigan),[43] and Dr. Michael Ward (NIH).[44] Two healthy control and two C9-NRE carrier hiPSC-i^{3}Neuron lines were obtained from Dr. Barmada, and one healthy control and one C9-NRE carrier hiPSC-i^{3}Neuron line were obtained from Dr. Michael Ward (NIH). The C9-NRE and healthy control lines are sex-balanced; two male lines and one female line per group. Further patient demographic information for each line is provided in Table S1. All hiPSCs were maintained in Essential 8 Flex media (Gibco) on Matrigel-coated plates (Corning). Differentiation was performed using the techniques outlined in.[44] Briefly, to differentiate iPS cells into cortical neurons, cells were dissociated into single cells and plated on Matrigel-coated plates in induction media (DMEM/F12, N2, NEAA, and L-glutamine) containing 2 mg/ml doxycycline. Cells were induced into neurons by treatment with doxycycline for 3 days before being dissociated and plated on PLO-coated plates. Cells were then allowed to mature for an additional 22 days in cortical maturation media consisting of BrainPhys media (STEMCELL) supplemented with BDNF (Peprotech), NT-3 (Peprotech), B27 (Gibco), and Laminin (Thermo Fisher), with half media changes twice weekly. Neurons were harvested or experimented upon at 25 days post-differentiation (3 days of induction, 22 days of maturation). The hiPSC-i^{3}Neuron lines were previously authenticated and characterized; i^{3}Neurons expressed pan-neuronal markers MAP2 (microtubule-associated protein 2), βIII-tubulin, and Tau during culturing and on the day of experimentation.[43,44] Each hiPSC-i^{3}Neuron line tested negative for mycoplasma contamination upon receipt and initial expansion.

Primary rat cortical cultures

All *in vitro* experiments involving the isolation of rodent cortical neurons were performed in accordance with the guidelines set forth by the Institutional Animal Care and Use Committees at Thomas Jefferson University. Embryonic day 16 (E16) rat embryos were harvested, brains were dissected, and the meninges were removed. The sex of animals used for primary cultures was not able to be determined at the developmental age of dissection. Cortices and midbrain regions were cut into small pieces with scissors and incubated on a shaker at 80 x g for 45 min at 37°C in 0.2% trypsin in HBSS without Ca^{2+} and Mg^{2+} (Cytiva). FBS (Cytiva) was added, and the cell suspension was centrifuged at 800 x g for 10 minutes at 4°C. Cells were washed with Ca^{2+} and Mg^{2+} free HBSS and centrifuged at 800 x g for 10 minutes at 4°C. The cell suspension was then passed through a 70 μm strainer (Foxx Life Sciences) to remove undigested connective tissue and large cellular clumps. Dispersed cells were then counted and plated in poly-D lysine-coated plates. Neurons were maintained in Neurobasal medium (Gibco) with B27 supplement (Gibco), with half media changes twice weekly. Experiments were performed on day *in vitro* 21.

METHOD DETAILS

KCl depolarization of neurons

Rat cortical neurons or i^{3}Neurons were silenced overnight (16 hours) with 1 μM TTX. The following day, neurons were stimulated with KCl depolarization buffer (170 mM KCl, 2 mM $CaCl_2$, 1 mM $MgCl_2$, 10 mM HEPES, solution pH 7.4)[49], by adding warmed depolarization buffer to media in a volume to achieve a final concentration of ~55mM KCl, or with an equal volume of media (vehicle treated). Neurons were depolarized for 0 hours (vehicle), 2 hours, or 6 hours and were harvested at each time point.

Calcium imaging

Rat cortical neurons or i^{3}Neurons were washed with aCSF (10 mM HEPES, 1 mM $MgCl_2$, 2 mM $CaCl_2$, 10 mM glucose, 145 mM NaCl, 5 mM KCl), and loaded with 1 μM Fluo-4 AM for 15 minutes. Neurons were then washed twice with aCSF and incubated for 5 minutes in between each wash prior to the start of recording. Neurons were imaged on a confocal microscope (Nikon A1R) with a 10x objective every 3 seconds for 10 minutes. A baseline recording of 2 mins was captured prior to perfusion of high-KCl containing buffer (10 mM HEPES, 1 mM $MgCl_2$, 2 mM $CaCl_2$, 10 mM glucose, 95 mM NaCl, 55 mM KCl). ROIs were captured using NIS Elements software. Normalized fluorescence values over time (ΔF/F) was calculated and the area under the curve (AUC) was calculated in GraphPad Prism 9.

Quantitative polymerase chain reaction (qPCR)

RNA was isolated using RNeasy Plus Mini Kit (Qiagen) and cDNA was synthesized from 500 ng RNA using a QuantiTect Reverse Transcription Kit (Qiagen). For rat cortical cultures, qPCR was performed using PowerUP SYBR Green (Thermo Fisher). Primer sequences are in Table S2. Beta-actin was used to normalize each target. For i^{3}Neurons, qPCR was performed using Taqman Assays (Table S3), and beta-actin was also used as a normalizer in these experiments.

Western blotting

Cells were scraped and collected from wells in RIPA buffer (150 mM NaCl, 1% Nonidet (NP-40), 0.5% deoxycholic acid, 0.1% sodium dodecyl sulfate, 50 mM Tris–HCl, 2 mM EDTA, and 1:100 protease inhibitor cocktail) at 4°C and then sonicated in a Diagenode Bioruptor for 10 cycles of 30 seconds on / 30 seconds off at 4°C. Samples were spun at 20,000 x g for 15 minutes at 4°C, and the supernatant was collected. Samples were quantified via BCA, and 10-20 μg per sample was loaded onto a 4-12% NuPAGE Bis-Tris gel (Invitrogen) for electrophoretic separation. Protein was transferred from the gel onto a Nitrocellulose membrane using the Trans-Blot Turbo Transfer System (BioRad). Membranes were then stained with Revert 700 Total Protein stain (LI-COR Biosciences) and imaged with a LI-COR Odyssey Imaging System (LI-COR Biosciences). Membranes were then blocked with 5% milk in PBS. Primary antibodies were incubated sequentially. We followed the experimental methods for probing C9orf72 similar to previous reports,[69] with slightly optimized modifications detailed here. For rat cortical neurons, the C9orf72 antibody GTX632041 (GT779, GeneTex, 1:1000) was incubated overnight in 5% BSA in 0.1% PBST. For i^{3}Neurons, the C9orf72 antibody GTX634482 (GT1553, GeneTex, 1:500) was incubated overnight in 5% BSA in 0.1% PBST. Washes were performed with 0.1 % PBST. Membranes were incubated with secondary antibodies (Thermo Fisher, 1:10,000) to detect C9orf72 primary antibodies for 1 hour at room temperature in 5% BSA in 0.1 % PBST. The primary antibody for c-Fos (9F6, Cell Signaling, 1:1000) was incubated overnight in 5% milk in 0.1% TBST. Washes were performed with 0.1 % TBST. Membranes were incubated with secondary antibodies (Thermo Fisher, 1:10,000) to detect c-Fos primary antibody for 1 hour at room temperature in 5% milk in 0.1 % TBST. Membranes were imaged using LI-COR Odyssey Imaging System (LI-COR Biosciences), and data analysis was performed using LI-COR Image Studio.

Survival assay

CellTox Green Dye (Promega) was added to culture media at a dilution of 1:1000 one day prior to depolarization experiments. 16 hours prior to the addition of KCl, cells were silenced with TTX. A baseline fluorescence reading was taken on a Citation5 plate reader (BioTek) to establish background prior to KCl addition. Cells were depolarized with KCl, and fluorescent readings were taken at 2 hours and 6 hours following depolarization.

Multi-electrode Array (MEA)

Cortical i^{3}Neurons were plated on a CytoView MEA plate (Axion Biosystems) at day 3 of differentiation. MEA recordings were performed on a Maestro Edge (Axion Biosystems) every 3-4 days during differentiation. Recordings on the MEA were performed prior to media changes. Neurons were removed from the incubator and were allowed to equilibrate in the recording chamber for 15 minutes prior to the start of recording. Neurons were recorded for 15 minutes, and the total number of spikes over the whole recording was reported.

QUANTIFICATION AND STATISTICAL ANALYSIS

All statistical analyses were performed using GraphPad Prism 9 software as described in each Figure legend. All data are shown as mean ± SEM. The value of *n*, what *n* represents, the statistical test used, and statistical significance is stated in each figure legend.